Evolutions of packing properties of perfect cylinders under densification and crystallization

Lufeng Liu, Ye Yuan, Wei Deng, and Shuixiang Li

Citation: The Journal of Chemical Physics **149**, 104503 (2018); doi: 10.1063/1.5049562
View online: https://doi.org/10.1063/1.5049562
View Table of Contents: http://aip.scitation.org/toc/jcp/149/10
Published by the American Institute of Physics

Evolutions of packing properties of perfect cylinders under densification and crystallization

Lufeng Liu, Ye Yuan, Wei Deng, and Shuixiang Li[a)]
Department of Mechanics and Engineering Science, College of Engineering, Peking University, Beijing 100871, China

(Received 23 July 2018; accepted 30 August 2018; published online 13 September 2018)

Cylindrical particles are ubiquitous in nature and industry, and a cylinder is a representative shape of rod-like particles. However, the disordered packing results of cylinders in previous studies are quite inconsistent with each other. In this work, we obtain the MRJ (maximally random jammed) packings and the MDRPs (maximally dense random packings) of perfect cylinders with the aspect ratio (height/diameter) $0.2 \le w \le 6.0$ using the ASC (adaptive shrinking cell) algorithm and the IMC (inverse Monte Carlo) method, respectively. The optimal aspect ratio corresponding to the maximal packing density is $w = 0.9$ in the MRJ state, while the value is $w = 1.2$ in the MDRP state. Then we investigate the evolutions of packing properties of perfect cylinders under densification and crystallization. We compare the different final packing states generated via the two methods with different compression rates and order constraints. In the densification procedure, we generate jammed and random packings of cylinders with various compression rates via the ASC and IMC method, respectively. When decreasing the compression rate, we find that the packing density increases but the optimal w remains the same in both methods. In the crystallization procedure, the order constraint in the IMC method is gradually released which means the degree of order in the packings is allowed to increase, and we find that the optimal w shifts from 1.2 to 0.9 while the packing density increases as well. Meanwhile, the random packings evolve into the jammed packings in the crystallization procedure which reflects the competition mechanism between the randomness and jamming. These results also indicate that the optimal w is solely related to the degree of order in the cylinder packings but not determined by the protocol or packing density. Furthermore, a uniform shape elongation effect on the random-packing densities of various shaped particles is found via a new proposed definition of the scaled aspect ratio. Finally, a rough linear relationship between the mean and standard deviation of the reduced Voronoi cell volumes is obtained only for the random packings. Our findings should lead to a better understanding toward the jammed and random packings and are helpful in guiding the granular material design. *Published by AIP Publishing.*
https://doi.org/10.1063/1.5049562

I. INTRODUCTION

Packings of rod-like particles are ubiquitous in nature and arise in a variety of applications. The packings of cylindrical particles attract great interest because of their wide application in chemical industry, liquid crystals, and fibrous materials. A cylinder is often characterized by the aspect ratio $w = L/D$, where L and D are the length and basal diameter, respectively. The densest known packing of cylinders in three-dimension space can be regarded as the densest ordered packing of circles in two-dimension, and the maximum packing density is $\pi/\sqrt{12} \approx 0.9069$.[1] Kusner found that the upper bounds of the packing density for circular cylinders with a high aspect ratio ($w \ge 48.3267$) are $\pi/\sqrt{12} + 5/w$, but they did not give the corresponding structure.[2] Meanwhile, the phase behaviors of cylinders change significantly with different aspect ratios. Veerman and Frenkel[3] found that disk-like cylinders with an aspect ratio of about 0.2 appeared to exhibit an orientationally ordered phase with a cubic symmetry, even though these particles themselves have a cylindrical symmetry. This phenomenon was also discussed by Duncan *et al.*,[4] and the phase diagram of short cylinders was given by Mejia.[5] To determine the optimal aspect ratio for which the packing might reach a cubatic phase, Blaak *et al.*[6] calculated the ratio of the excluded volumes of perpendicular and parallel orientation and found the minimum at $w \approx 0.886$. They also found that freely rotating cylinders with $w = 0.9$ exhibited the cubic phase with a weak but significant, fourfold orientational order. However, this structural phase transition is not first order,[6] and the dense packings for slender cylinders exhibit a nematic phase.[7,8]

The disordered packings of cylinders have been systematically studied via experiments,[9–21] simulations,[14,18,21–28] and theoretical studies[11,29,30] since 1970s. The aspect ratio w of the cylinders studied varies from 0.1 to 100, and some common conclusions have been drawn. As shown in Fig. 1, the

a)Author to whom correspondence should be addressed: lsx@pku.edu.cn

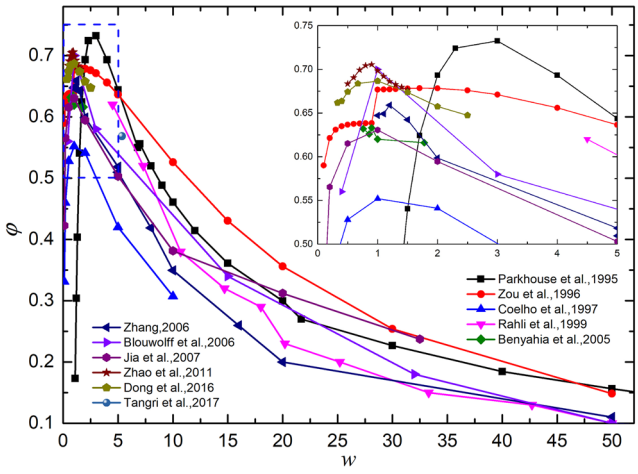

FIG. 1. The densities of disordered packings of cylinders in previous studies. The inset shows the details of the rectangular region surrounded by blue dashed lines.

packing density φ first increases with the increase of w for disk-like cylinders ($w < 0.7$). Then the φ reaches a maximum near the shape of an equilateral cylinder ($w = 1.0$), but the peak location of φ is not uniform between these studies. Finally, the φ decreases with the increase of w for slender cylinders ($w > 3.0$). Especially, the density of the random close packing (RCP) of the equilateral cylinder ($w = 1.0$) was within 0.6–0.71,[10,12,15–17,25,27] as a result of the ambiguous definition of the RCP. Furthermore, some theoretical and empirical formulas were given to predict the disordered-packing densities of disk-like or slender cylinders. From the liquid-crystal theory, Evans and Gibson[29] presented a basic formula for the RCP densities of slender cylinders as $\varphi = k/w$, where k is a constant. Theoretical computations showed that $k = 4$, while a fit to available experimental data gave $k = 5.3$. Philipse[30] also deduced this basic formula from the perspective of the excluded volumes, and the constant k in their work was about 5.4. Parkhouse and Kelly[11] used a combination of geometric, probabilistic, and empirical arguments to obtain a general formula for the random-packing densities of slender cylinders in the form $\varphi = 2\ln(w)/w$. Zou and Yu[12] correlated the experimental data as a function of particle sphericity ψ (defined as the ratio of the surface area of a sphere having the same volume as the particle to the surface area of the particle) and obtained an empirical equation for the porosities $\varepsilon = 1 - \varphi$ of loose and dense disordered packing of cylinders ($w > 1.0$) and disks ($w < 1.0$).

However, the optimal aspect ratio w, where the maximal φ is obtained, is still not well discussed. As can be seen in the inset of Fig. 1, the results from literature studies are confused. It is difficult to obtain the optimal w via experiments because of their low precision and high cost. With computer simulations, Zhang[24] used a collective rearrangement (CR) algorithm to obtain the dense random packings of cylinders, and they found the maximal $\varphi \approx 0.6589$ at $w = 1.2$. However, Zhao *et al.*[26] found the maximal $\varphi \approx 0.7055$ at $w = 0.9$ via an improved relaxation algorithm. We can see the distinct values of the optimal aspect ratio corresponding to the maximal packing density in these studies. Meanwhile, the packing densities of Zhang's results are much lower than those of Zhao's work for all the aspect ratios, and the degrees of order of the packings in these two studies are different as well. No obvious global or local orders are observed in the cylinder packings with $w \le 2.0$ obtained by Zhang. While the cylinder packings with w near 1.0 obtained by Zhao *et al.* are locally cubatic ordered, even no global nematic order is observed. Therefore, what is the main factor that induces to the different optimal aspect ratios? The protocol, packing state, packing density, or degree of order? More work need to be carried out to explain why their results are not the same and find the optimal aspect ratio corresponding to the maximal packing density of cylinders, which has significant meanings in many industrial applications.

Moreover, in recent studies,[31,32] we found uniform aspect ratio effects, i.e., shape elongation and compression effects, on the random-packing densities of symmetric particles with three equal cross sections when $w = 1.0$, such as the spherocylinders,[33] spheroids,[34] cuboids,[31] and superellipsoids.[32,35,36] All the packing density versus w curves of these particles are in "M" type with the minimum at $w = 1.0$ and maximum at $w \approx 0.7$, 1.5, if the packings are in highly disordered states. However, for the disordered packings of cylinders, the packing density curve is single-peaked and the optimal aspect ratio corresponding to the maximal packing density is 0.9[26] or 1.2[24] in previous studies. The aspect ratio effects on the packing densities for cylinders are significantly different from those particles mentioned above. Therefore, the influence of particle shape on the aspect ratio effects is still not clear. Is there any general relationship between the aspect ratio effects and the particle shape?

Finally, the Voronoi analysis[37] of non-spherical particle packings becomes more popular in recent studies. Their results showed that the probability distribution functions (PDFs) of the local packing density (or the reduced local Voronoi cell volume) in the random packings of ellipsoid,[27,38] cylinder,[27] and superellipsoid[32] are in normal[32,38] or log-normal[27] distributions. Furthermore, the standard deviations of these distributions depend only on the global packing density and are not related to the aspect ratios.[27,32,38] A linear function was used to fit their relationships, which can be used to predict the random-packing densities of different shaped particles.[32,38] Dong *et al.*[27] carried out the Voronoi tessellation of mechanically stable cylinder packings with different sliding friction coefficients. They systemically studied the effects of aspect ratio and friction coefficient on the Voronoi cells in terms of the reduced volume, reduced surface area, and sphericity, including the forms of PDFs, their means, and standard deviations. An exponential function was used to fit the relationship between the standard deviation of reduced Voronoi cell volume and the global packing density, which was used to predict the Voronoi cell properties of cylinder packings. However, the Voronoi cell properties for the packings of hard frictionless cylinders in specific packing states need to be reviewed and compared.

In this work, we obtain the Maximally Random Jammed (MRJ) packings and Maximally Dense Random Packings (MDRPs) of cylinders with the aspect ratio $0.2 \le w \le 6.0$. Both the MRJ state and the MDRP state are the modifications of the RCP state proposed by Bernal.[39] The MRJ packing is

maximally random (quantified by specified order metrics with the smallest value) among all jammed packings. Here "jammed" means that each particle (except rattlers) cannot be moved, while all of the other particles in the system are fixed as originally discussed in Ref. 40, which is the definition of "local jamming."[41] The MDRP is defined as the densest packing in the random state in which the particle positions and orientations are randomly distributed.[31–33,42] The packing density of the MDRP corresponds to a sharp transition in the order map, which characterizes the onset of nontrivial spatial correlations among the particles.[33,42] The MDRP is also regarded as a glass state of hard particle systems with an artificial constraint and is always random.[31] The jammed or mechanically stable condition is emphasized in the MRJ state, while the random condition is emphasized in the MDRP state. For the particle shapes which are difficult to crystalize, the packing density of the MDRP is close to that of the RCP or MRJ packing, such as the spheroids,[32] spherocylinders,[33] octahedra,[42] and superellipsoids with small surface shape parameters.[32] However, for the particle shapes which are easy to crystalize, the MDRP is highly disordered but may not be jammed with a lower packing density, while the MRJ packing possesses some local or global ordered structures as a result of keeping jammed, such as the cuboids[31] and superellipsoids with large surface shape parameters.[32]

The adaptive shrinking cell (ASC) algorithm[43,44] and the inverse Monte Carlo (IMC) method[31,32] are, respectively, utilized to generate the MRJ packings and MDRPs of cylinders in this work. The ASC algorithm is a Monte Carlo (MC) compression process with random particle movements and allows the simultaneous change of different lattice vectors of the simulation box at the same time. The IMC method is based on the ASC method with an order constraint to prevent the forming of ordered structures in the packing. We find that the optimal aspect ratio corresponding to the maximal packing density is $w = 0.9$ in the MRJ state, while the value is $w = 1.2$ in the MDRP state, consistent with the results of Zhao[26] and Zhang,[24] respectively. Meanwhile, the values of order parameters demonstrate that some ordered structures arise in the MRJ packings, while the MDRPs are always highly disordered. Therefore, the reason why these results about the location of the maximal packing density are not the same is that the packings they obtained are not in the same state and have different levels of order. A competition mechanism between the randomness and jamming plays an important role in the cylinder packings.

Then we investigate the evolutions of packing properties of perfect cylinders under densification and crystallization. We compare the different final packing states generated via the two methods with different compression rates and order constraints. In the densification procedure, we generate a series of packings with decreasing the compression rate in the algorithms, and we find that the packing density increases but the optimal w corresponding to the maximal packing density remains the same. Meanwhile, the jammed packings of cylinders with different aspect ratios possess various local ordered structures, which can also be detected by the order parameters. While the random packings are always highly disordered with very small values of order parameters and no obvious ordered structures can be observed. In the crystallization procedure, the order constraint in the IMC packing method is gradually released which means more degree of order in the packings is allowed, and we find that the optimal w shifts from 1.2 to 0.9, while the packing density increases as well. Moreover, the random packing evolves into the jammed packing in the crystallization procedure and the randomness is sacrificed to keep the packing jammed, which reflects the competition mechanism between the randomness and jamming. These results also indicate that the optimal w is solely related to the degree of order in the cylinder packings but not determined by the protocol or packing density.

Furthermore, via the new proposed scaling factor R_s and the scaled aspect ratio w_s, the location ($w_s \approx 1.5$) of the maximal random-packing density of cylinders ($R_s = 4/\pi$) is consistent with that of symmetric particles having three equivalent main axes ($R_s = 1.0$, such as spherocylinders,[33] spheroids,[34] cuboids,[31] and superellipsoids[32,35,36]), which indicates a uniform shape elongation effect on the random-packing densities of different shaped particles. Finally, the Voronoi tessellations of the jammed and random packings of cylinders are carried out, and a rough linear relationship between the mean and standard deviation of the reduced Voronoi cell volumes is obtained only for the random packings. Our findings should lead to a better understanding toward the jammed and random packings.

The rest of the paper is organized as follows: in Sec. II, we introduce the perfect cylinder model and the overlap detection algorithm, then we describe the order parameters and the packing algorithms we use. The simulation results are discussed in Sec. III, and concluding remarks are provided in Sec. IV.

II. METHODOLOGY

In this part, we introduce the perfect cylinder model and the overlap detection algorithm, then we describe the order parameters and the packing algorithms we use.

A. The perfect cylinder model and overlap detection

The cylindrical model we apply in this work is an ideal accurate model with sharp edges. A cylindrical particle consists of a cylindrical face and two disk faces. The overlap detection between two identical cylinders in the packing systems is carried out in three steps. First, a rough detection based on the background grid, circumscribed sphere, and inscribed sphere of the cylinder is used to mostly avoid the complicated and precise overlap detection. Then the infinite and finite cylindrical face to face test is carried out analytically, as well as the disk to disk test. Finally, the disk to cylindrical face test, involving a numerical optimization to find the closest point on the disk to the axis of the cylindrical face, is carried out. More details can be seen in Refs. 45–48.

B. The order parameters

1. *The global orientational order parameters*

In this work, we use the nematic order parameter S_2, the order parameters I_2, and I_4 to evaluate the global orientational

order in different forms. The nematic order parameter S_2 is an important and widely used metric which characterizes the physical properties of the nematic state. The S_2 is the largest eigenvalue of the orientational alignment matrix $\boldsymbol{Q}$ which is defined as[49]

$$\boldsymbol{Q} = \frac{1}{N}\sum_{i=1}^{N}\left(\frac{3}{2}\hat{u}_i\hat{u}_i^T - \frac{1}{2}\boldsymbol{I}\right), \tag{1}$$

where $\hat{u}_i$ is the principal axis which is the unit column vector of the axial direction of cylinder i, $\boldsymbol{I}$ is the unit matrix, and N is the total number of particles in the system. Furthermore, the order parameters I_2 and I_4 are defined based on the modified spherical harmonics[6]

$$I_l = \sqrt{\frac{4\pi}{2l+1}\sum_{m=-l}^{m=l}\left|\frac{1}{N}\sum_{i=1}^{N}Y_l^m(\theta_i,\varphi_i)\right|^2}, \quad l = 2,\ 4, \tag{2}$$

where θ_i and φ_i are the polar and azimuthal angles of the principal axis $\hat{u}_i$ and $Y_l^m(\theta,\ \varphi)$ are the spherical harmonics. S_2 measures the uniaxial order only, I_2 measures the combination of uniaxial and biaxial order, while I_4 is able to measure the uniaxial, biaxial, and cubatic order. The values of S_2, I_2, and I_4 are all in the range of [0,1]. In a random packing with 200 particles, the values of S_2, I_2, and I_4 are all around 0.1. For a packing in which all the particles are parallel to each other, i.e., uniaxial order, all these three global orientational order parameters are equal to unity. In a configuration with biaxial order, the I_2 and I_4 are large, while the S_2 is small. While in a cubatic phase, i.e., a configuration with three axial orders, only the I_4 is large, while the S_2 and I_2 are small.

2. The normalized local cubatic order parameter S_{4local}

The normalized local cubatic order parameter S_{4local} is similar to the local cubatic order parameter defined by Zhang *et al.*[16] and is applied to evaluate the degree of local orientational order of local structures with different sizes. First, the average orientation correction of particles with n nearest neighbor particles is evaluated by $S_{4local,n}$ which is defined as[41]

$$S_{4local,n} = \frac{1}{N}\sum_{i=1}^{N}\left[\frac{1}{8n}\sum_{j=1}^{n}\left(35\cos^4\theta_{ij} - 30\cos^2\theta_{ij} + 3\right)\right], \tag{3}$$

where n = 1, 2, 3, ..., 26 represents the number of particles which are closest to the ith particle, $\cos\theta_{ij} = \hat{u}_i \cdot \hat{u}_j$ is the inner product of the principal axes of particle i and its jth neighbor particle. We choose 26 as the maximal number of n because there are 26 neighbor particles around a particle in the simple cubic (SC) lattice packing and 26 is large enough, as is particularly stated in Ref. 31. Moreover, according to the central limit theorem, the probability distribution functions of $S_{4local,n}$ in the random state are in Gaussian distributions, the mean $S^{\mu}_{4local,n} = 0.0$ and the standard deviation $S^{\sigma}_{4local,n}$ are linear to $1/\sqrt{Nn}$,

$$S^{\mu}_{4local,n} = 0.0,\ S^{\sigma}_{4local,n} = 1/\left(3\sqrt{Nn}\right), \tag{4}$$

which is also verified by the Monte Carlo tests.[31] Then the $\tilde{S}_{4local,n}$ is normalized as

$$\tilde{S}_{4local,n} = \left|\frac{S_{4local,n} - S^{\mu}_{4local,n}}{S^{\sigma}_{4local,n}}\right| = \left|3\sqrt{Nn}S_{4local,n}\right| \tag{5}$$

and the normalized local cubatic order parameter S_{4local} is

$$S_{4local} = \max_n\left\{\tilde{S}_{4local,n}|n = 1,2,3,\ldots,26\right\}. \tag{6}$$

For a uniaxial ordered packing of cylinders, both the global orientational order parameters mentioned above and the $S_{4local,n}$ are unity, and the normalized local cubatic order parameter S_{4local} is larger than 150.0 for N = 200. However, in a polycrystalline structure or a quasi-random packing[50] with large amounts of local ordered clusters, the global orientational order parameters are small, while the S_{4local} is large. The smaller the S_{4local} is, the more random the packing is. In an ideal random packing, S_{4local} = 0.0.

3. The normalized local bond-orientational order parameter Q_{6local}

The normalized local bond-orientational order parameter Q_{6local} is based on the original bond-orientational order parameter[51] Q_6 and is used to evaluate the local bond-orientational order in a packing configuration. The calculation of Q_{6local} is described in Ref. 32 in detail. Like the $S_{4local,n}$, the average bond-orientational correlation of particles with n nearest neighbor particles is evaluated by $Q_{6local,n}$,

$$Q_{6local,n} = \sqrt{\frac{4\pi}{13}\sum_{m=-6}^{m=6}\left|\frac{1}{N}\sum_{i=1}^{N}\left[\frac{1}{n}\sum_{j=1}^{n}Y_{6m}\left(\theta_{ij},\varphi_{ij}\right)\right]\right|^2}, \tag{7}$$

where $\theta_{ij}, \varphi_{ij}$ are the polar and azimuthal angles of the bond formed by particle i and its jth neighbor particle. Here we also choose 26 as the maximal number of n for the reasons mentioned above. Via the Monte Carlo tests of $Q_{6local,n}$,[32] we find that the values of $Q_{6local,n}$ in the random state are also in Gaussian distributions, the mean $Q^{\mu}_{6local,n}$ and standard deviation $Q^{\sigma}_{6local,n}$ are linear to $1/\sqrt{Nn}$ with

$$Q^{\mu}_{6local,n} = 0.981\,23/\sqrt{Nn},\quad Q^{\sigma}_{6local,n} = 0.193\,79/\sqrt{Nn}. \tag{8}$$

The $\tilde{Q}_{6local,n}$ is normalized as

$$\tilde{Q}_{6local,n} = \left|\frac{Q_{6local,n} - Q^{\mu}_{6local,n}}{Q^{\sigma}_{6local,n}}\right| \tag{9}$$

and the normalized local bond-orientational order parameter Q_{6local} is

$$Q_{6local} = \max_n\left\{\tilde{Q}_{6local,n}|n = 1,2,3,\ldots,26\right\}. \tag{10}$$

The Q_{6local} is larger than 60.0 in the Simple Cubic (SC), Body-Centered Cubic (BCC), Face-Centered Cubic (FCC), and Hexagonal Close-Packed (HCP) packings. The smaller the Q_{6local} is, the more random the packing is. In an ideal random packing, Q_{6local} = 0.0.

C. The packing algorithms

1. The adaptive shrinking cell method

The adaptive shrinking cell (ASC) method was devised by Torquato and Jiao to obtain the densest packings[43,44] and the MRJ packings[52] of ideal hard polyhedral particles. The ASC algorithm is a Monte Carlo (MC) compression process with random particle movements and allows the simultaneous change of different lattice vectors of the simulation box at the same time. In a MC move step, each particle is randomly moved (translated or rotated) for λ times, then a boundary deformation (compression or shear) is carried out. The boundary is a parallelepiped with periodical boundary conditions in three directions. If all the particles are still non-overlapped after a particle movement or a boundary deformation, the movement or deformation is accepted. Otherwise, it is rejected. Starting from an unjammed packing with a very low packing density ($\varphi \approx 0.1$), MC move steps are applied to the particulate system until the particles cannot be moved with the moveable scale smaller than 1×10^{-5}. The packing density and degree of order of the final packing configuration are affected by the compression rate Γ which is defined as the inverse of λ, $\Gamma = 1/\lambda$. Especially, Chen *et al.* used the ASC numerical scheme to investigate the equilibrium phase behavior and the MRJ state of truncated tetrahedra with different compression rates.[53] More details about the ASC algorithm can be found in Refs. 41, 43, 44, 52, and 53. In this work, we set the compression rate Γ = 0.001, 0.01, 0.02, 0.1, 1.0 to obtain the jammed cylinder packings with different packing densities and degrees of order. In general, the smaller the compression rate Γ is, the slower the particulate system will be compressed. The final packings will be denser and more ordered. As also stated in Ref. 53, for a very small Γ, the system is compressed slowly and the particles are moved adequately to form ordered structures. The system almost behaves in an equilibrium process and will finally evolve into a highly dense and ordered packing. While for a larger Γ, the system is compressed much faster and is driven out of the equilibrium branch. The particles do not have enough time to form ordered structures and are jammed quickly. Therefore, the system will eventually turn into a disordered and jammed packing with a lower packing density.

We also note that the specific compression rate for the true MRJ state of cylinders may vary with the aspect ratio. According to Refs. 52 and 53, and in order to decrease the computation costs and compare the MRJ packings with the MDRPs of cylinders for convenience, we just consider the cylinder packings obtained with $\Gamma = 0.1$ as approximations to the MRJ states, namely, the MRJ-like packings. We note that the MRJ packings referred in this work are actually the MRJ-like packings.

2. The inverse Monte Carlo method

The inverse Monte Carlo (IMC) method[31,32] allows one to generate a maximally dense packing of hard particles with a controllable random degree evaluated by prescribed order parameters. This method is based on the ASC method mentioned above. In the IMC method, the particles are also randomly translated or rotated and the boundary is allowed to compress but not shear. Therefore, the boundary is fixed to be cubic with periodical boundary conditions in three directions. Besides the non-overlapping condition, the particle movement and boundary deformation are also rejected if all the calculated order parameters are larger than a prescribed value Op^{up}, which is regarded as an order constraint. The IMC method will degenerate into the ASC method if $Op^{up} = +\infty$. The Op^{up} is set to be small enough ($Op^{up} = 0.5$) to prevent the formation of ordered structures. Therefore, the system is always random and becomes a supercooled liquid, turning into glass. Meanwhile, the final packing density is also affected by the compression rate Γ. The smaller the Γ is, the denser the final packing will be. However, the degree of order of the final configurations is mainly determined by the order constraint Op^{up} rather than the compression rate Γ. More details are discussed in Refs. 31 and 32.

In this work, we use the normalized local cubatic order parameter S_{4local} and the normalized local bond-orientational order parameter Q_{6local} mentioned above to control the degrees of local orientational and bond-orientational order, respectively. In order to obtain the closely approximate MDRPs of cylinders, the order constraint Op^{up} is set to be 0.5, which is small enough to ensure the randomness of the system, and the compression rate Γ is set to be 0.001, which is small enough to ensure that the final packing is maximally dense on the premises of randomness. Moreover, a strong linear relationship exists between the final packing density and the Op^{up} when the Op^{up} is smaller than 4.0.[31] Therefore, the packing density when $Op^{up} = 0.0$, which means the packing density of the ideal MDRP, can be predicted via a linear fitting. In order to decrease the computer costs and compare the other packing properties, we just use the final packings obtained with $Op^{up} = 0.5$ as close approximations to ideal MDRPs. Meanwhile, we also set $\Gamma = 0.001$, 0.01, 0.02, 0.1, 1.0 and $Op^{up} = 0.5$, 3.0, 5.0, 10.0, 20.0, 30.0 to investigate the effects of compression rate and order constraint, respectively.

III. RESULTS AND DISCUSSION

As introduced in the method part, we generate the MRJ packings and MDRPs of cylinders with different aspect ratios w via the ASC method and the IMC method, respectively. We also investigate the evolutions of packing properties of perfect cylinders under densification and crystallization. In the densification procedure, we generate a series of jammed and random packings with decreasing the compression rate Γ in both methods. In the crystallization procedure, we release the order constraint Op^{up} in the IMC method with $\Gamma = 0.02$. The total number of particles is set to be $N = 200$, which is large enough to ignore the system size effect.[31,32,42] All the packings of cylinders are averaged over 5 times and the error bars in the figures below represent the standard deviations. Some finial packing structures of the jammed and random packings generated with different compression rates Γ are shown in Figs. 2 and 3, respectively. The packings generated with different order constraints Op^{up} are shown in Fig. 4. The details are discussed below.

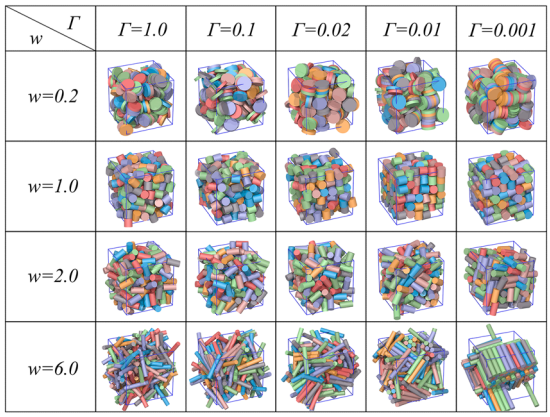

FIG. 2. The evolutions of the jammed packing configurations of cylinders generated via the ASC method with the aspect ratio $w = 0.2, 1.0, 2.0, 6.0$ and the compression rate $\Gamma = 0.001, 0.01, 0.02, 0.1, 1.0$. All the cylinder packings with different w become more ordered with the decrease of Γ. The packings generated with $\Gamma = 0.1$ are the MRJ packings.

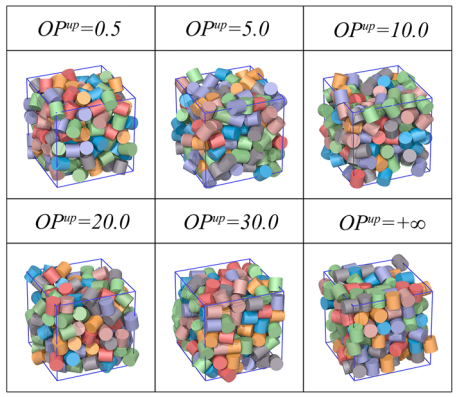

FIG. 4. The evolution of the packing configurations of cylinders generated via the IMC method with the aspect ratio $w = 1.0$, the compression rate $\Gamma = 0.02$, and the order constraint $Op^{up} = 0.5, 5.0, 10.0, 20.0, 30.0$. The packing configuration of cylinders generated via the ASC method with $w = 1.0$, $\Gamma = 0.02$ is also shown at the bottom right and is titled by $Op^{up} = +\infty$. The cylinder packings become more ordered with the increase of Op^{up}.

A. MRJ packings and MRDPs of cylinders

As mentioned in the methodology part, the MRJ packings of cylinders are the jammed packings obtained via the ASC method with $\Gamma = 0.1$ and the MDRPs of cylinders are the random packings obtained via the IMC method with $\Gamma = 0.001$, $Op^{up} = 0.5$. Figure 5(a) shows the packing densities of the MRJ packings and the MDRPs of cylinders as a function of the aspect ratio. The simulation results of Zhang[24] and Zhao[26] are also demonstrated in the figure for comparison. The maximal φ of the MRJ packing is obtained at $w = 0.9$, while the maximal φ of the MDRP is obtained at $w = 1.2$, consistent with the results of Zhao[26] and Zhang,[24] respectively. For $w \le 1.0$, the packing density of the MRJ packings is higher than that of the MDRPs. While for $w \ge 1.2$, the packing density of the MDRPs is little higher.

Meanwhile, as can be seen in Figs. 5(b)–5(f), the global order parameters S_2 and I_2 are always smaller than 0.15 for both the MRJ packings and MDRPs of cylinders with different aspect ratios. However, the I_4, S_{4local}, and Q_{6local} for the MRJ packings of cylinders are much higher than those for the MDRPs, especially for the cylinders with w near 0.2 and 1.0. In other words, the MRJ packings are not always strictly random packings, as can also be seen in Fig. 2. In the MRJ packings, the randomness may be sacrificed and particles tend to crystalize to keep the packings jammed or mechanically stable. A competition mechanism between the randomness and jamming plays an important role in the cylinder packings and will be discussed later.

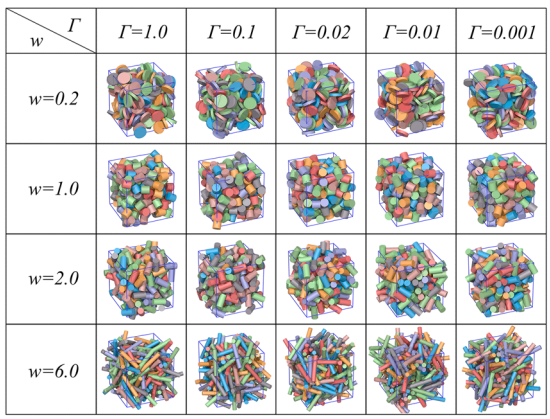

FIG. 3. The evolutions of the random packing configurations of cylinders generated via the IMC method with the aspect ratio $w = 0.2, 1.0, 2.0, 6.0$, the compression rate $\Gamma = 0.001, 0.01, 0.02, 0.1, 1.0$, and the order constraint $Op^{up} = 0.5$. All the cylinder packings with different w are highly disordered with different Γ. The packings generated with $\Gamma = 0.001$ are the MDRPs.

Therefore, the reason why the results of Zhao[26] and Zhang[24] about the locations of maximal packing density are not the same is that the packings they obtained are not in the same state and have different order levels. The cylinders with w near 0.2 and 1.0 are easy to crystalize. Meanwhile, the packing densities of Zhao's results are very close to those of the MRJ packings obtained in this work. However, the packing densities of Zhang's results are much lower than those of the MDRP state. This is probably because the packing they obtained is a kind of random packing but not the maximally dense one via the CR algorithm, while the MDRP state is the maximally dense state among all random packings.

We also compare the aspect ratio effects on the random-packing densities of cylinders with those of other shaped particles. In Refs. 31 and 32, we found uniform aspect ratio effects on the random-packing densities of symmetric particles with three equal cross sections when $w = 1.0$, such as spherocylinders,[33] spheroids,[34] cuboids,[31] and superellipsoids.[32,35,36] All the packing density versus w curves of these particles are in "M" type with the minimum at $w = 1.0$ and the maximum at $w \approx 0.7, 1.5$. However, for the MDRPs of cylinders, the packing density curve is single-peaked and the maximum is obtained at $w \approx 1.2$. We note that these symmetric particles mentioned above have the same cross and vertical sections when $w = 1.0$ and the definition of aspect ratio is uncontroversial. Nevertheless, a cylinder with $w = 1.0$ has distinct cross and vertical sections which are circle and square, respectively. Considering the differences mentioned above, we scale the aspect ratio as

$$w_s = R_s w, \tag{11}$$

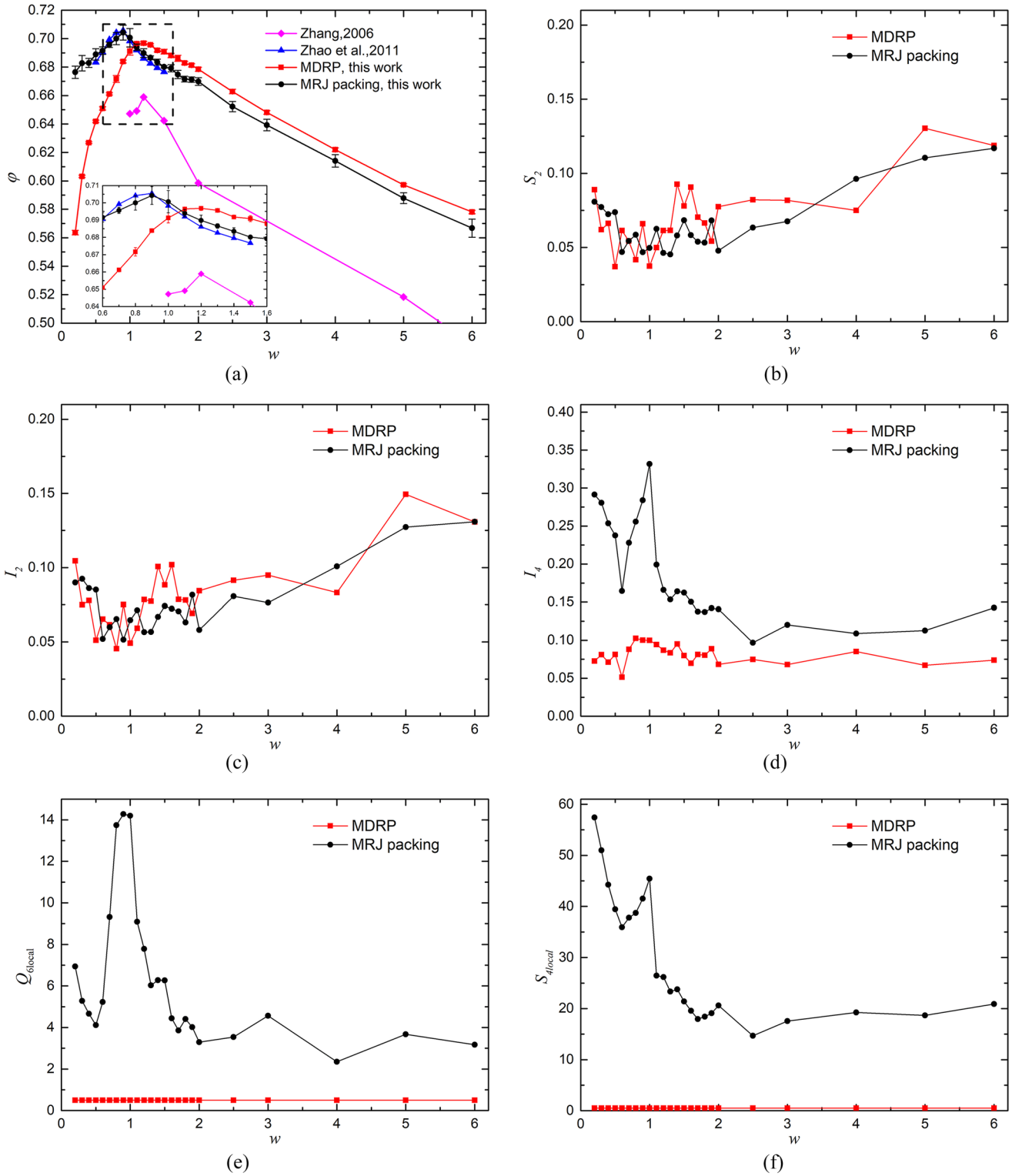

FIG. 5. The packing density φ (a), the global orientational order parameters S_2 (b), I_2 (c), I_4 (d), the normalized local cubatic order parameter S_{4local} (e), and the normalized local bond-orientational order parameter Q_{6local} (f) of the MRJ packings and MDRPs of cylinders with $0.2 \le w \le 6.0$. The simulation results of Zhang[24] and Zhao[26] are also shown for comparison in (a). The inset in (a) shows the details of the rectangular region surrounded by black dashed lines. The maximum density of the MRJ packings and Zhao's results is at $w = 0.9$, while the maximum density of the MDRPs and Zhang's results is at $w = 1.2$. The I_4, S_{4local}, and Q_{6local} for the MRJ packings of cylinders are much higher than those for the MDRPs, especially for the cylinders with w near 0.2 and 1.0.

where w_s is the scaled aspect ratio, R_s is the scaling factor which is defined as the ratio of the vertical sectional area to the cross-sectional area when $w = 1.0$.

For spherocylinders, spheroids, cuboids and superellipsoids, whose cross and vertical sections are equal when $w = 1.0$, the scaling factor $R_s = 1.0$. While for cylinders, the

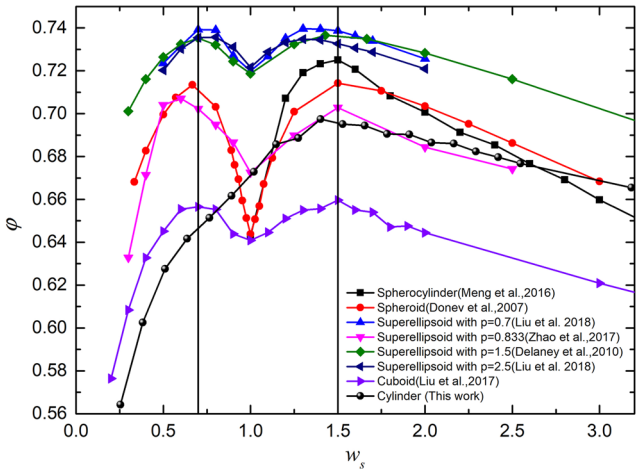

FIG. 6. The packing densities of different shaped particles as a function of the scaled aspect ratio w_s. All the packing density curves obtain a maximum at $w_s \approx 1.5$, indicating a uniform shape elongation effect.

scaling factor $R_s = 4/\pi$. Then the packing density curves of these particles are redrawn as a function of w_s in Fig. 6. The location of the maximum of cylinders is also $w_s \approx 1.5$, which is consistent with other shaped particles. When $w_s > 1.0$, the packing densities of all these particles first increase until reaching the maximal value at $w_s \approx 1.5$ and then decrease, indicating a uniform shape elongation effect on the random-packing densities of particles with different R_s. However, when $w_s < 1.0$, the packing density of cylinders always decreases with the decrease of w_s, while the packing densities of other shaped particles first increase and then decrease. Therefore, the shape compression effects on the random-packing densities of particles with different R_s may not be the same and more work will be carried out to find their relations in the future.

B. Evolutions under densification

1. The evolutions of the jammed packings

The evolutions of the packing density φ, the global orientational order parameters S_2, I_2, I_4, the normalized local cubatic order parameter S_{4local}, and the normalized local bond-orientational order parameter Q_{6local} of the jammed packings generated via the ASC method with $\Gamma = 0.001$, 0.01, 0.02, 0.1, 1.0 are shown in Figs. 7(a)–7(f), respectively. Figure 7(a) shows that all the cylinder packings with different w become denser with the decrease of Γ which means the reduction of the compression rate. During the densification process, the packing density of cylinders with $w = 0.9$ is always a local maximum whichever Γ is used. When $\Gamma = 1.0, 0.1$, the packing density curve is single peaked. However, the packing densities of cylinders with $w = 0.2$, 6.0 are also relatively high when Γ is even smaller. Meanwhile, during the densification process, obvious ordered structures arise in the jammed packings of cylinders with different aspect ratios, as can also be seen in Fig. 2.

For the disk-like cylinders with $w < 0.5$, the I_4 and S_{4local} increase rapidly and the Q_{6local} increases little slower with the decrease of Γ. However, the values of S_2 and I_2 are always near 0.1, which are small enough to verify that no global nematic order arises in these packings. Therefore, the disk-like cylinders tend to form stacks of two to five particles with disk-disk face joint and these stacks tend to be perpendicular to each other, indicating a cubatic phase. The stacks become longer and more perpendicular with each other with the decrease of Γ, and no nematic phase is observed, as can be seen in Fig. 2.

For the cylinders near the shape of an equilateral cylinder with $0.7 < w < 1.3$, the I_4, S_{4local}, and Q_{6local} increase sharply and become more prominent with the decrease of Γ. The S_2 and I_2 are always near 0.1 for $\Gamma \geq 0.01$. While for $\Gamma = 0.001$, the S_2 and I_2 also become prominent and larger than 0.2 but smaller than 0.4. This is because the main axes of these cylinders are almost along three directions perpendicular to each other, which also causes the small increase of S_2 and I_2. Therefore, the cylinders near the shape of an equilateral cylinder tend to form a cubatic phase with their centers in a simple cubic lattice and their main axes along three directions perpendicular to each other. No nematic phase is observed as well, as can be seen in Fig. 2.

For the slender cylinders with $w \geq 3.0$, the S_2, I_2, I_4, and S_{4local} increase with the decrease of Γ. Meanwhile, these order metrics increase with the increase of w. The Q_{6local} is always small for $\Gamma \geq 0.01$, while the Q_{6local} increases rapidly for $\Gamma = 0.001$, indicating the arising of high bond-orientational order. Therefore, the slender cylinders tend to form a nematic phase and the centers of slender cylinders tend to be arranged in order as well, as also shown in Fig. 2.

Finally, we note that even for the fastest compression process with $\Gamma = 1.0$, not all the packings of cylinders with $0.2 \leq w \leq 6.0$ are fully random. As can be seen in Figs. 7(d)–7(f), the I_4 approaches 0.2 and the S_{4local} approaches 40 for the disk-like cylinders. The Q_{6local} is also little higher for the cylinders near the shape of an equilateral cylinder. The results indicate that the randomness in the cylinder packings must be sacrificed to keep the packings jammed or mechanically stable for the disk-like cylinders and the cylinders near the shape of an equilateral cylinder. These kinds of cylinders are easy to crystalize.

2. The evolutions of the random packings

Figures 8(a)–8(f) show the evolutions of the packing density φ, the global orientational order parameters S_2, I_2, I_4, the normalized local cubatic order parameter S_{4local}, and the normalized local bond-orientational order parameter Q_{6local} of the random packings generated via the IMC method with the compression rate $\Gamma = 0.001$, 0.01, 0.02, 0.1, 1.0 and the order constraint $Op^{up} = 0.5$. As can be seen in Fig. 8(a), all the cylinder packings with different w also become denser with the decrease of Γ.

However, during the densification process, all the packing density curves are always single peaked and the locations of the peaks are all about $w = 1.2$ whichever Γ is used. The packing densities of the random packings are lower than those of the jammed packings shown above with the same Γ and the locations of the peaks are different from those of the jammed packings. These differences are caused by a competition mechanism between the randomness and jamming,

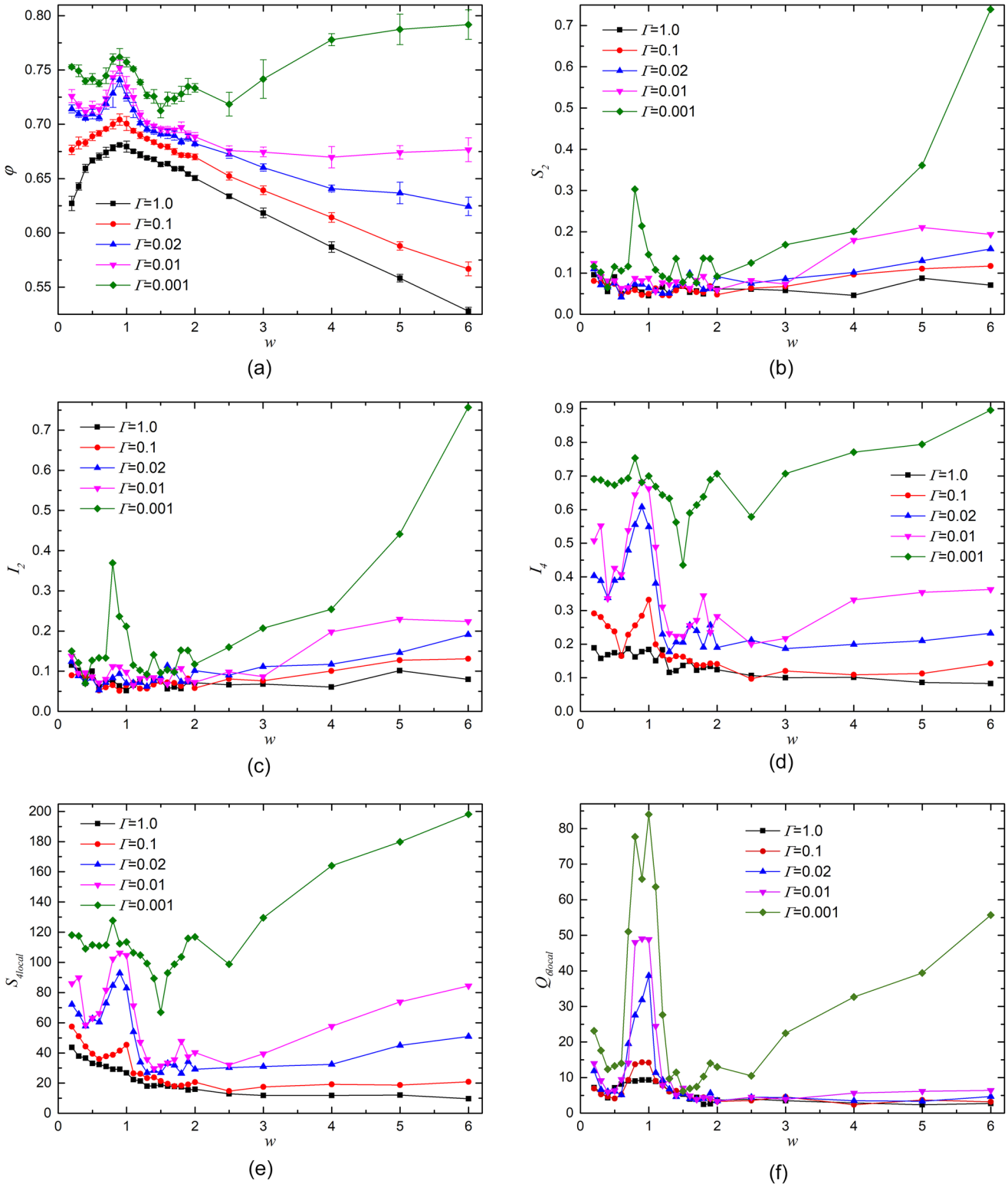

FIG. 7. The evolutions of the packing density φ (a), the global orientational order parameters S_2 (b), I_2 (c), I_4 (d), the normalized local cubatic order parameter S_{4local} (e), and the normalized local bond-orientational order parameter Q_{6local} (f) of the jammed packings generated via the ASC method with the compression rate $\Gamma = 0.001, 0.01, 0.02, 0.1, 1.0$. The packing density of cylinders with $w = 0.9$ is always a local maximum whichever Γ is used. The order parameters increase with the decrease of Γ.

which will be discussed in Sec. III C. Moreover, no matter which compression rate Γ is applied, all the global order parameters S_2, I_2, and I_4 are around 0.1 and the local order parameters S_{4local} and Q_{6local} are almost 0.5 during the densification process, as a result of the small value of the order constraint $Op^{up} = 0.5$. Therefore, all the packings generated via this method are highly disordered, as also demonstrated in Fig. 3.

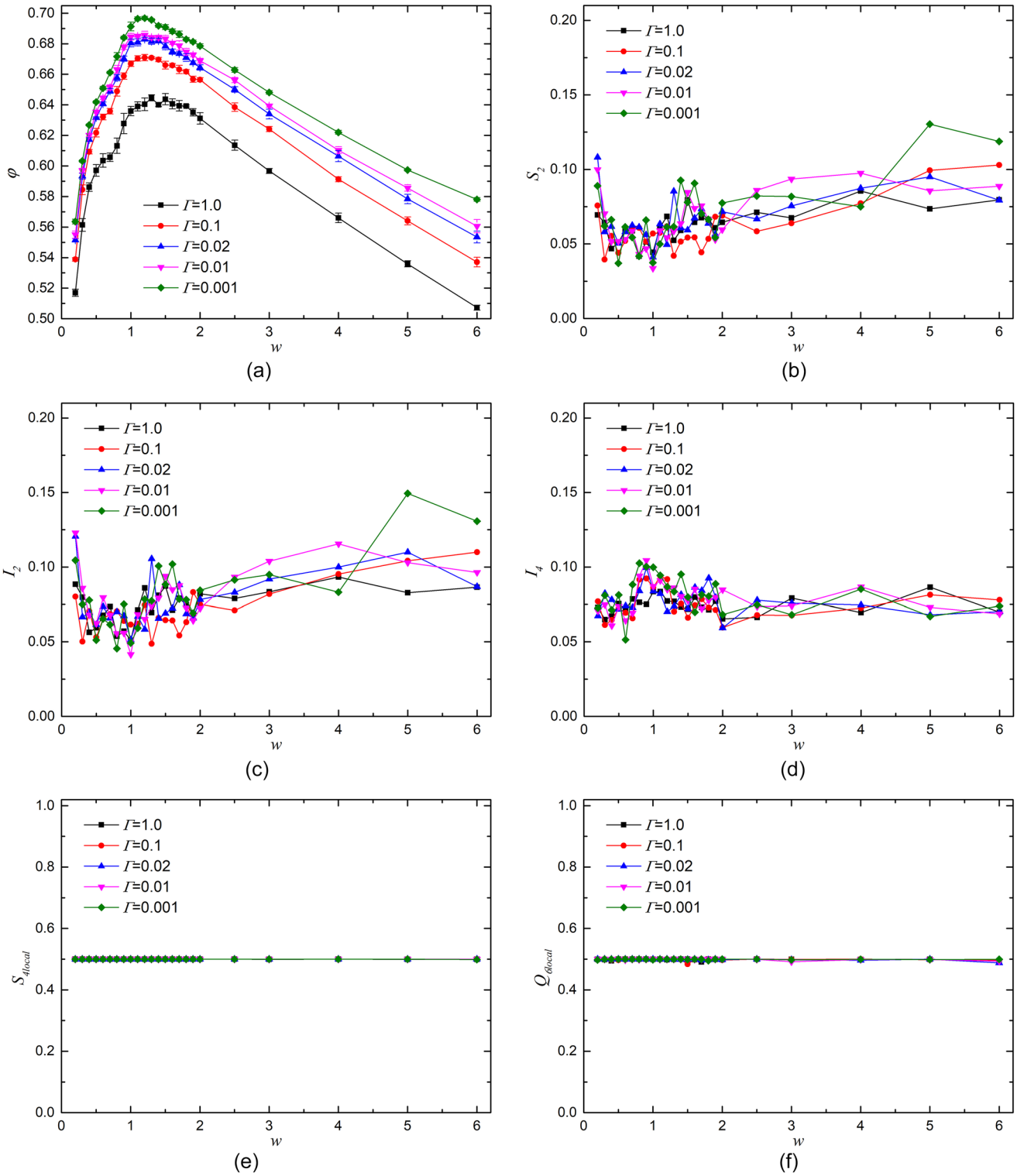

FIG. 8. The evolutions of the packing density φ (a), the global orientational order parameters S_2 (b), I_2 (c), I_4 (d), the normalized local cubatic order parameters S_{4local} (e), and the normalized local bond-orientational order parameters Q_{6local} (f) of the random packings generated via the IMC method with the compression rate Γ = 0.001, 0.01, 0.02, 0.1, 1.0 and the order constraint Op^{up} = 0.5. The packing density curves are always single peaked and the locations of the peaks are always about w = 1.2. Meanwhile, the order parameters are always very small in these random packings.

C. Evolutions under crystallization

As mentioned above, the packing density at w = 0.9 is a local maximum on the packing density curves of the jammed packings, while the maximal packing density for the random packings accrues at w = 1.2. The difference is caused by a competition mechanism between the randomness and jamming. Via the ASC method, the packings are compressed into jammed configurations and some local ordered structures appear in order to keep the packings jammed. Meanwhile,

with the decrease of the compression rate Γ, the local ordered structures become more dominant and the packings become denser and more ordered. By comparison, in the IMC method with a small value of the order constraint $Op^{up} = 0.5$, the packings are compressed on the premise of randomness and the crystallization is suppressed. With the decrease of the compression rate Γ, the packings are densified but still keep random.

In order to investigate the effects of the order constraint, i.e., the evolutions of packings under crystallization, we gradually release the order constraint which means more ordered structures in the packings are allowed in the evolutions. Thus, the packings tend to crystallize and a compromise between the randomness and jamming is carried out. The order constraint is set to be $Op^{up} = 0.5, 3.0, 5.0, 10.0, 20.0, 30.0, +\infty$. If $Op^{up} = +\infty$, the order constraint is completely released and the IMC method will degenerate into the ASC method. The compression rate is set as $\Gamma = 0.02$ for simplification. Figures 9(a)–9(f) show the packing density φ, the global orientational order parameters S_2, I_2, I_4, the normalized local cubatic order parameter S_{4local}, and the normalized local bond-orientational order parameter Q_{6local} of the cylinder ($0.6 \le w \le 1.6$) packings generated with different values of Op^{up}.

As can be seen in Fig. 9(a), the packing densities of cylinders with different aspect ratios w increase with the increase of Op^{up}. Meanwhile, all the packing density curves with $0.6 \le w \le 1.6$ are single peaked and the location of the peak gradually shifts from $w = 1.2$ (the peak location of the random packings) to $w = 0.9$ (the peak location of the jammed packings). Moreover, the S_2, I_2 are always near 0.1 which are very small, but the I_4, S_{4local}, and Q_{6local} increase sharply. Especially, the S_{4local} almost reaches the Op^{up}. The maxima of I_4 and S_{4local} are at $w = 0.9$. However, the Q_{6local} reaches the maximum at $w = 1.0$, because the centers of the equilateral cylinders are easier to form a simple cubic lattice. Therefore, releasing the order constraint makes the packings denser and more ordered. The particulate system is transformed from a random packing to a jamming packing, as can also be seen in Fig. 4. The randomness is sacrificed to keep the packing jammed and the cylinders with w near 1.0 are easy to crystalize.

The optimal aspect ratio for the MRJ packing is about 0.9. On one hand, the cylinders with $w \approx 0.9$ are easier to crystalize. As can be seen in Fig. 7, the values of order metrics at $w \approx 0.9$ are always local maxima. Therefore, in order to keep jammed and maximal random, the MRJ packing of cylinders with $w \approx 0.9$ is more ordered than those with other aspect ratios and achieves a higher packing density. On the other hand, both the minimal relative excluded volume and the minimal ratio of the excluded volumes of perpendicular and parallel orientation are obtained at $w = \sqrt{\pi}/2 \approx 0.886$, which is very close to 0.9. This may also be a reason why the optimal aspect ratio for the MRJ packing is $w \approx 0.9$. The optimal aspect ratio for the MDRP is about 1.2. This is because the randomness condition is specially required and the MDRP of cylinders with w near 0.9 is not jammed and the packing density of the MDRP is much lower than that of the MRJ packing, as can be seen in Fig. 5. As a compromise between the randomness and densification, the optimal aspect ratio for the MDRP is about 1.2, which is consistent with the optimal aspect ratio values of other rod-like particles via the scaled aspect ratio with $w_s \approx 1.5$. However, we still have no idea about the reason why the optimal scaled aspect ratio for the MDRPs of rod-like particles is about 1.5 rather than the other value. More work will be carried out in the future.

To summarize, the optimal aspect ratio w corresponding to the maximal packing density is not influenced by the compression rate Γ in both packing methods. When the Γ is decreased, the packing density φ increases but the optimal w does not change. However, the optimal w is influenced by the order constraint Op^{up} in the IMC method. When the Op^{up} is released, the packing density φ also increases but the optimal w shifts from the peak location of random packings ($w = 1.2$) to the peak location of jammed packings ($w = 0.9$). These results also indicate that the optimal w is solely related to the degree of order in the cylinder packings but not determined by the protocol or packing density. Moreover, we conjecture that the effects of degree of order on the value of optimal w are also valid for other shaped particles whose MDRP and MRJ packing are not the same, such as cuboids. More work will be carried out in the future to verify the conjecture.

D. The Voronoi analysis

Recent studies show that the probability distribution functions (PDFs) of the local packing density (or the reduced local Voronoi cell volume) in the random packing configurations of ellipsoid,[27,38] cylinder,[27] or superellipsoid[32] are in normal or log-normal distributions. Moreover, the standard deviations of these distributions depend only on the global packing density and are not related to the aspect ratios. A linear (or an exponential) function is used to fit their relationships, which can be used to predict the random-packing densities of different shaped particles. In this work, we also tessellate the jammed and random packing configurations of hard frictionless cylinders generated above and investigate their microcosmic properties via the set Voronoi diagram method.[54] The cylinder surface is discretized via the cylindrical coordinates, and the Voro++ program[55] is used to compute the Voronoi cells of discrete points. We carry out the Voronoi analysis via the reduced local Voronoi cell volume V_{local} which is defined as

$$V_{local} = \frac{V_{cell}}{V_p}, \tag{12}$$

where V_p is the volume of the particle in the cell and V_{cell} is the volume of the particle's Voronoi cell. Here we use the reduced local Voronoi cell volume V_{local} rather than the local packing density $1/V_{local}$ because the mean of V_{local} is accurately equal to the inverse of the global packing density, while the mean of the local packing density is not accurately equal to the global packing density. We mainly focus on the PDF form, the mean V^{μ}_{local}, and the standard deviation V^{σ}_{local} of V_{local}.

Figure 10(a) shows the discretized surfaces of cylinders with $w = 0.2, 1.0, 2.0, 6.0$. The points are uniformly distributed on the cylindrical surfaces. The polar angles and radial

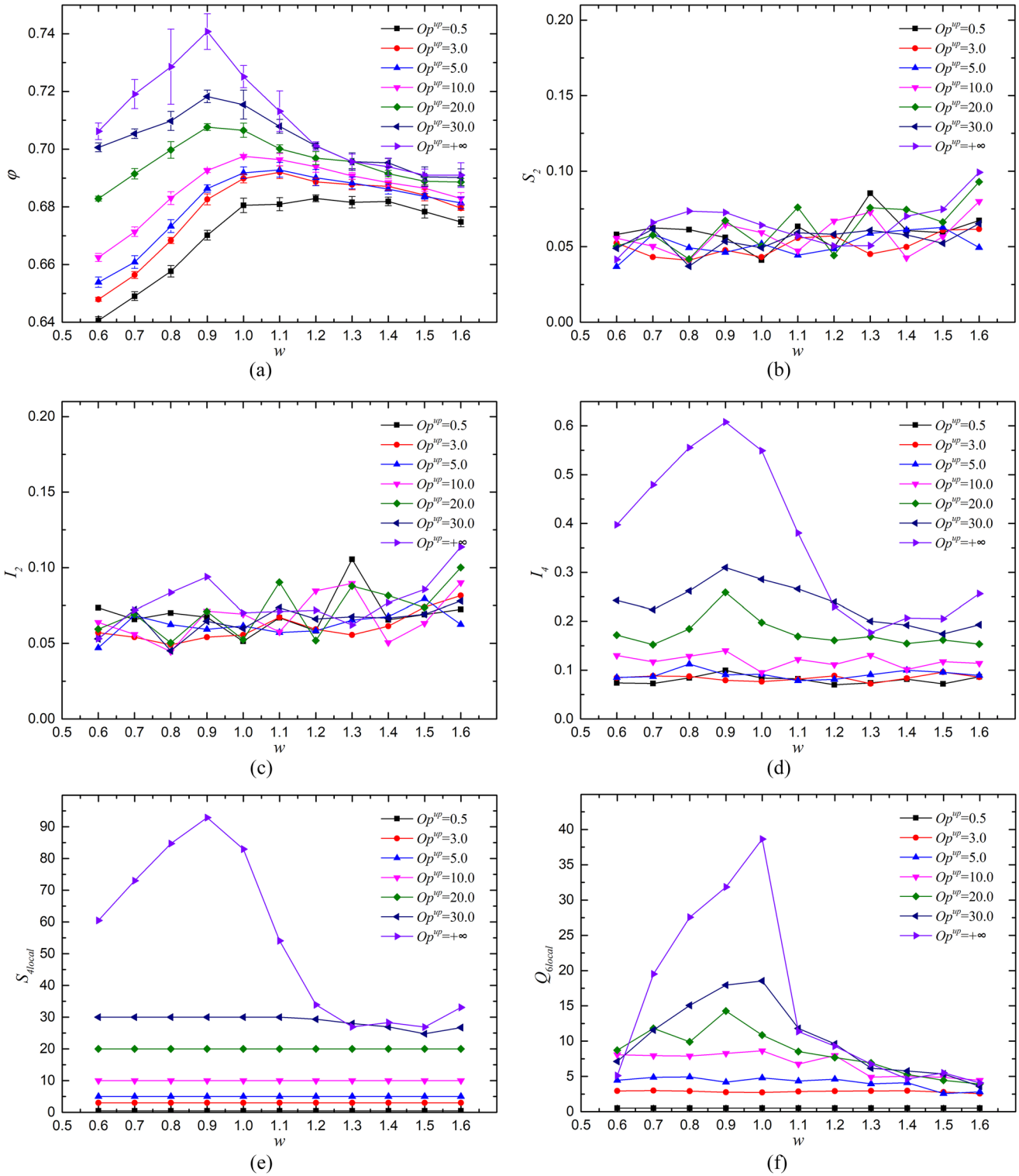

FIG. 9. The evolutions of the packing density φ (a), the global orientational order parameters S_2 (b), I_2 (c), I_4 (d), the normalized local cubatic order parameter S_{4local} (e), and the normalized local bond-orientational order parameter Q_{6local} (f) of the packings generated via the IMC method with the compression rate $\Gamma = 0.02$ and the order constraint Op^{up} = 0.5, 3.0, 5.0, 10.0, 20.0, 30.0, +∞. The peak of the packing density curve shifts from $w = 1.2$ to $w = 0.9$ and the I_4, S_{4local}, and Q_{6local} increase with the increase of Op^{up}. While the S_2 and I_2 are always very small.

distances of the points on the disk surface are also uniformly distributed. All the cylinder surfaces are discretized by nearly 1000 points to ensure the accuracy of the Voronoi tessellation. Figure 10(b) shows the relative errors of the V^{σ}_{local} as a function of the resolution which is the number of points used to discretize the surface. Here the jammed packings of cylinders with $w = 0.2$, 1.0, 6.0, $\Gamma = 0.01$ are used to validate the resolution. The relative errors of V^{σ}_{local} decrease rapidly with the increase of the resolution, and the errors are generally smaller than 2.0% when about 1000 points are used. However, the

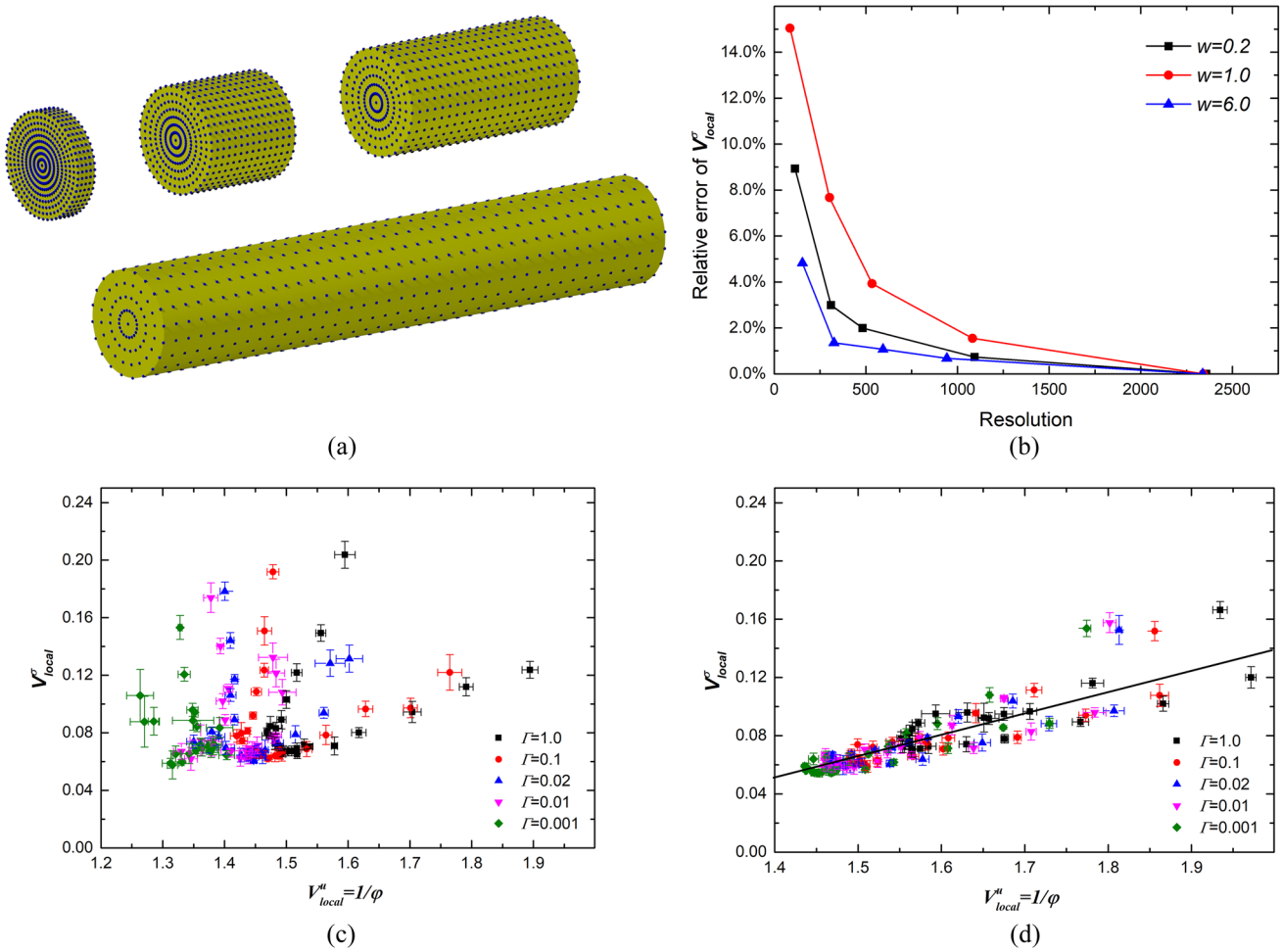

FIG. 10. (a) The discretized surfaces of cylinders with w = 0.2, 1.0, 2.0, 6.0. The cylinder surfaces are discretized by 1094, 1082, 1058, 942 points, respectively. (b) The relative errors of the V^{σ}_{local} as a function of the resolution. The jammed packings of cylinders with w = 0.2, 1.0, 6.0, Γ = 0.01 are used to validate the resolution. The errors decrease rapidly with the increase of the resolution and are generally smaller than 2.0% if about 1000 points are used. (c) The relationship between the mean V^{μ}_{local} and standard deviation V^{σ}_{local} for the jammed packing configurations of cylinders with different aspect ratios w and compression rates Γ. No obvious relationship is observed. (d) The relationship between the mean V^{μ}_{local} and standard deviation V^{σ}_{local} for the random packing configurations of cylinders with different aspect ratios w and compression rates Γ. A rough linear relationship is observed.

computational cost increases rapidly as the resolution increases. As a compromise between accuracy and computational cost, we use about 1000 points to discrete the surfaces of all the cylinders studied in this work.

The relationship between the mean V^{μ}_{local} and standard deviation V^{σ}_{local} calculated from the jammed and random packing configurations of cylinders with different w and Γ is shown in Figs. 10(c) and 10(d), respectively. The relationship between the V^{σ}_{local} and V^{μ}_{local} for the jammed packings is very chaotic, while a rough linear relationship is found for the random packings. Meanwhile, we also observe that the PDFs of V_{local} for all the random packings are in normal-like distributions, while only the PDFs for the jammed packings with very small or very large order-parameter values are in normal-like distributions. This is because all the particles are in similar random surroundings for all the random packings and the jammed packings with very small order parameters. For the jammed packings with very large order parameters, all the particles are in similar ordered surroundings. Therefore, the PDFs for these packings are in normal-like distributions. However, for other jammed packings which are partially ordered, some particles are in the random surroundings while others are in the ordered surroundings. Thus their PDFs are not in the normal distribution form. Therefore, in order to get a uniform relationship between the V^{σ}_{local} and V^{μ}_{local}, the packings must be on the same random degree, which shows the benefits of the MDRP state.

IV. CONCLUSION

In this work, we investigate the evolutions of the packing properties of perfect cylinders under densification and crystallization. First, the MRJ packings and MDRPs of cylinders with different aspect ratios are generated via the ASC and the IMC method, respectively. The global and local order parameters are used to evaluate the degree of order of these packings. The optimal aspect ratio corresponding to the maximal packing density is w = 0.9 in the MRJ state, while the value is w = 1.2 in the MDRP state, consistent with the results of Zhao[26] and Zhang,[24] respectively. Then we investigate the evolutions of packing properties of perfect cylinders under densification and crystallization.

In the densification procedure, the jammed and random packings are separately generated via the two methods with decreasing the compression rate. We find that all the packings become denser but the optimal w corresponding to the maximal packing density remains the same. Meanwhile, some local ordered structures arise in the jammed packings, while the random packings are always highly disordered. This is because of the competition mechanism between the randomness and jamming, which is investigated by gradually releasing the order constraint in the IMC method, i.e., the crystallization procedure.

In the crystallization procedure, the optimal w shifts from 1.2 to 0.9, while the packing density and the degree of order increase with the releasing of the order constraint. Meanwhile, the random packing evolves into the jammed packing in this procedure, and the randomness is sacrificed to keep the packings jammed. The competition mechanism explains the differences of the literature results about the optimal aspect ratios. The packings they obtained are not in the same order level, and the cylinders with w near 1.0 are easy to crystalize. Zhang's results are highly random with lower packing densities, while Zhao's results have some local ordered structures and higher packing densities. These results also indicate that the optimal w is solely related to the degree of order in the cylinder packings but not determined by the protocol or packing density.

Moreover, we propose the concept of the scaling factor R_s and the scaled aspect ratio w_s, which are successfully used to draw a uniform shape elongation effect on the random-packing densities of various shaped particles. The random-packing density first increases with the increase of w_s from $w_s = 1.0$ and reaches a maximal value at $w_s \approx 1.5$ for all the rod like particles such as spherocylinders, spheroids, cuboids, superellipsoids, and cylinders. However, the shape compression effects on the random-packing densities of particles with different scaling factors R_s are not identical and more work will be carried out in the future to investigate the relation between the surface shape and the shape compression effects. We also note that the uniform aspect ratio effects discussed here must be on the premise of randomness rather than jamming or mechanical stability. In the MRJ or RCP state, the aspect ratio effects still work for the particle shapes which are difficult to crystalize, such as spherocylinders, spheroids, and superellipsoids with small surface shape parameters, whose MRJ or RCP state is almost the same with the MDRP state. However, for particle shapes which are easy to crystalize, such as cuboids, superellipsoids with large surface shape parameters and cylinders studied in this work, the aspect ratio effects for the MRJ or RCP state are not uniform. Therefore, the MDRP state provides a better platform which shows the uniform particle shape effects on the random-packing densities.

Finally, we carried out the Voronoi tessellations for the jammed and random cylinder packing configurations via the set Voronoi diagram method. A rough linear relationship between the mean and standard deviation of the reduced Voronoi cell volumes is obtained for the random packings. However, the relationship for the jammed packings is chaotic. Meanwhile, the PDFs of the reduced Voronoi cell volume for all the random packings are in normal-like distributions, while only the PDFs for jammed packings with very small or very large order parameter values are in normal-like distributions. These findings further show the benefits of the MDRP state. Moreover, further studies should be carried out to investigate the exact form of the PDFs of the reduced Voronoi cell volume for systems in various states. Our findings should lead to a better understanding toward the jammed and random packings and are helpful in guiding the development of theoretical models for particle packings as well as the granular material design.

ACKNOWLEDGMENTS

This work was supported by the National Natural Science Foundation of China (Grant Nos. 11272010, 11572004, and U1630112), the Science Challenge Project (Grant No. JCKY2016212A502), and the High-performance Computing Platform of Peking University.

[1] A. Trovato, X. T. Hoang, and J. R. Banavar, Proc. Natl. Acad. Sci. U. S. A. **104**, 19187 (2007).
[2] W. Kusner, Discrete Comput. Geom. **51**, 964 (2014).
[3] J. A. C. Veerman and D. Frenkel, Phys. Rev. A **45**, 5632 (1992).
[4] P. D. Duncan, M. Dennison, A. J. Masters, and M. R. Wilson, Phys. Rev. E **79**, 031702 (2009).
[5] A. F. Mejia, Y. Chang, R. Ng, M. Shuai, M. S. Mannan, and Z. Cheng, Phys. Rev. E **85**, 061708 (2012).
[6] R. Blaak, D. Frenkel, and B. M. Mulder, J. Chem. Phys. **110**, 11652 (1999).
[7] M. C. Duro, J. A. Martin-Pereda, and L. M. Sese, Phys. Rev. A **37**, 284 (1988).
[8] T. Kuriabova, M. D. Betterton, and M. A. Glaser, J. Mater. Chem. **20**, 10366 (2010).
[9] J. V. Milewski, Composites **4**, 258 (1973).
[10] A. G. Dixon, Can. J. Chem. Eng. **66**, 705 (1988).
[11] J. G. Parkhouse and A. Kelly, Proc. R. Soc. A **451**, 737 (1995).
[12] R. Zou and A. Yu, Powder Technol. **88**, 71 (1996).
[13] O. Rahli, L. Tadrist, and R. Blanc, C. R. Acad. Sci., Ser. IIb: Mec., Phys., Astron. **327**, 725 (1999).
[14] G. Lumay and N. Vandewalle, Phys. Rev. E **70**, 051314 (2004).
[15] F. Benyahia and K. E. O'Neill, Part. Sci. Technol. **23**, 169 (2005).
[16] W. Zhang, K. E. Thompson, A. H. Reed, and L. Beenken, Chem. Eng. Sci. **61**, 8060–8074 (2006).
[17] J. Blouwolff and S. Fraden, Europhys. Lett. **76**, 1095 (2006).
[18] R. Caulkin, X. Jia, C. Xu, M. Fairweather, R. A. Williams, H. Stitt, M. Nijemeisland, S. Aferka, M. Crine, A. Léonard, D. Toye, and P. Marchot, Ind. Eng. Chem. Res. **48**, 202 (2009).
[19] M. J. Baker, P. G. Young, and G. R. Tabor, Comput. Chem. Eng. **35**, 1969 (2011).
[20] X. Zhang, C. Xia, X. Xiao, and Y. Wang, Chin. Phys. B **23**, 044501 (2014).
[21] H. Tangri, Y. Guo, and J. S. Curtis, Powder Technol. **317**, 72 (2017).
[22] K. E. Evans and M. D. Ferrar, J. Phys. D: Appl. Phys. **22**, 354 (1989).
[23] D. Coelho, J. F. Thovert, and P. M. Adler, Phys. Rev. E **55**, 1959 (1997).
[24] W. Zhang, "Experimental and computational analysis of random cylinder packings with applications," Ph.D. dissertation (Louisiana State University, Baton Rouge, 2006).
[25] X. Jia, M. Gan, R. A. Williams, and D. Rhodes, Powder Technol. **174**, 10 (2007).
[26] J. Zhao, S. Li, P. Lu, L. Meng, T. Li, and H. Zhu, Powder Technol. **214**, 500 (2011).
[27] K. Dong, C. Wang, and A. Yu, Chem. Eng. Sci. **153**, 330 (2016).
[28] Q. Qian, L. Wang, X. An, Y. Wu, J. Wang, H. Zhao, and X. Yang, Powder Technol. **325**, 151 (2018).
[29] K. E. Evans and A. G. Gibson, Compos. Sci. Technol. **25**, 149 (1986).
[30] A. P. Philipse, Langmuir **12**, 1127 (1996).
[31] L. Liu, Z. Li, Y. Jiao, and S. Li, Soft Matter **13**, 748 (2017).
[32] L. Liu, Z. Yu, W. Jin, Y. Yuan, and S. Li, Powder Technol. **338**, 67 (2018).
[33] L. Meng, Y. Jiao, and S. Li, Powder Technol. **292**, 176 (2016).

[34]A. Donev, R. Connelly, F. H. Stillinger, and S. Torquato, Phys. Rev. E **75**, 051304 (2007).
[35]G. W. Delaney and P. W. Cleary, Europhys. Lett. **89**, 34002 (2010).
[36]R. Yang, R. Zou, and A. Yu, Phys. Rev. E **65**, 041302 (2002).
[37]G. F. Voronoi, J. Reine Angew. Math. **136**, 67 (1909).
[38]F. M. Schaller, M. Neudecker, M. Saadatfar, G. W. Delaney, G. E. Schröder-Turk, and M. Schröter, Phys. Rev. Lett. **114**, 158001 (2015).
[39]J. D. Bernal, Nature **183**, 141 (1959).
[40]S. Torquato, T. M. Truskett, and P. G. Debenedetti, Phys. Rev. Lett. **84**, 2064 (2000).
[41]S. Torquato and F. H. Stillinger, Rev. Mod. Phys. **82**, 2633 (2010).
[42]L. Liu, P. Lu, L. Meng, W. Jin, and S. Li, Physica A **444**, 870 (2016).
[43]S. Torquato and Y. Jiao, Phys. Rev. E **80**, 041104 (2009).
[44]S. Torquato and Y. Jiao, Nature **460**, 876 (2009).
[45]J. Ketchel and P. Larochelle, in *Proceedings of the 2006 IEEE International Conference on Robotics and Automation* (IEEE, Orlando, Florida, 2006).
[46]N. Ibarra-Avalos, A. Gil-Villegas, and A. Martinez Richa, Mol. Simul. **33**, 505 (2007).
[47]M. Kodam, R. Bharadwaj, J. Curtis, and B. Hancock, Chem. Eng. Sci. **65**, 5852 (2010).
[48]V. Salnikov, D. Choï, and P. Karamian-Surville, Comput. Mech. **55**, 127 (2015).
[49]M. P. Allen, Liq. Cryst. **8**, 499 (1990).
[50]S. Li, P. Lu, W. Jin, and L. Meng, Soft Matter **9**, 9298 (2013).
[51]P. J. Steinhardt, D. R. Nelson, and M. Ronchetti, Phys. Rev. B **28**, 784 (1983).
[52]Y. Jiao and S. Torquato, Phys. Rev. E **84**, 041309 (2011).
[53]D. Chen, Y. Jiao, and S. Torquato, J. Phys. Chem. B **118**, 7981 (2014).
[54]F. M. Schaller, S. C. Kapfer, M. E. Evans, M. J. F. Hoffmann, T. Aste, M. Saadatfar, K. Mecke, G. W. Delaney, and G. E. Schröder-Turk, Philos. Mag. **93**, 3993 (2013).
[55]C. H. Rycroft, Chaos **19**, 041111 (2009).